Robust hydro-thermal power system controller considering energy capacitor system and wind power source

Thongchart Kerdphol*, Yaser Soilman Qudaih, Khairudin H. Basri and Yasunori Mitani

Department of Electrical and Electronics Engineering,
Kyushu Institute of Technology,
1-1, Sensui-cho, Tobata-ku, Kitakyushu-shi,
Fukuoka, 804-8550, Japan
Email: n589504k@mail.kyutech.jp
Email: yaser_qudaih@yahoo.com
Email: khai_hasan@yahoo.com
Email: mitani@ele.kyutech.ac.jp
*Corresponding author

Abstract: This paper presents the method to design the robust controller for the hydro thermal system considering interconnection of two areas. The feasibility of using the automatic generation control with energy capacitor system is implemented to both areas. Wind turbines are considered to be one of the most used alternative sources of energy to solve global warming worldwide. The output of wind turbines depends on the weather condition which causes large fluctuation in the power output when WTs connect to the system. So, the system should be capable of handling uncertainties caused by the wind turbines and load variations. H_∞ loop-shaping method is designed as the proposed controller which is used to regulate and improve system stability in the hydro thermal power system. Results demonstrate that the hydro thermal system with ECS-based H_∞-controller gives higher system stability and more robustness than the hydro thermal system with ECS-based PID controller.

Keywords: energy capacitor system; ECS; H_∞-LSDP; power system oscillation; robust control; wind energy.

Reference to this paper should be made as follows: Kerdphol, T., Qudaih, Y.S., Basri, K.H. and Mitani, Y. (2015) 'Robust hydro-thermal power system controller considering energy capacitor system and wind power source', *Int. J. Process Systems Engineering*, Vol. 3, Nos. 1/2/3, pp.90–109.

Biographical notes: Thongchart Kerdphol received his BEng and MEng from Kasetsart University, Bangkok, Thailand in 2010 and 2012. Currently, he is pursuing his DEng degree at Kyushu Institute of Technology. His research interests are in the area of the application of artificial intelligence in power systems, power system stability, smart grid, renewable energy, power system dynamics and controls.

Yaser Soilman Qudaih graduated from the University of Engineering and Technology, Lahore, Pakistan in 1996 as an Electrical Engineer. He completed his MSc and PhD degrees from Kumamoto University, Japan in Electrical Engineering. He is currently a Researcher (Project Assistant Professor) at the Department of Electrical Engineering and Electronics, Kyushu Institute of

Technology (KIT), Japan. His research interests are in the area of the application of artificial intelligence in power systems, power system stability, dynamics and controls and smart grid.

Khairudin H. Basri received his ST (equal to BSc degree) from Sriwijaya University, Palembang, Indonesia and MSc from The University of Manchester (formerly UMIST), UK in 1995 and 1999, respectively. Currently, he is pursuing in DEng degree at Kyushu Institute of Technology, Japan. His research interests are in the area of the application of artificial intelligence in power systems, power system stability, dynamics and controls and smart grid. He is a student member of IEEE.

Yasunori Mitani received his BSc, MSc and DEng in Electrical Engineering from Osaka University, Japan in 1981, 1983 and 1986, respectively. He was a Visiting Research Associate at the University of California, Berkeley, from 1994 to 1995. He is currently a Professor at the Department of Electrical Engineering and Electronics, Kyushu Institute of Technology (KIT), Japan. At present, he is the Head of Environmental Management Center of KIT. His research interests are in the areas of analysis and control of power systems. He is a member of the Institute of Electrical Engineers of Japan and IEEE.

This paper is a revised and expanded version of a paper entitled 'Robust hydro thermal power system controller considering energy capacitor system and wind power source' presented at the IEEE on Smart Energy Grid Engineering (SEGE'14), UOIT, Oshawa, Canada, 11–13 August 2014.

1 Introduction

Currently, many countries have increased their capacity to generate electricity from renewable sources (Gu et al., 2011; Francisco et al., 2015). The main target is to reduce the amount of CO_2 injected to the atmosphere and to eliminate the greenhouse effect mainly caused by the huge consumption of fossil oil. Wind energy is one of the renewable energies used broadly because it is sustainable energy and environmental friendly. The numbers of installed wind power sources are increasing around the world. However, the wind power output affected by environmental change and weather condition. So, wind energy is not used as main energy sources because the electrical power obtained from the wind energy is fluctuating which leads to the oscillation of power system frequency (Lalor et al., 2005). In this case, the H_∞ loop-shaping design procedure (H_∞-LSDP) controller is proposed to the system in order to handle such a power fluctuation.

On the other hand, an energy storage device with a fast response time can be installed to power system in order to decrease the frequency oscillations caused by random load scheme. Various energy storage devices have been designed and presented in the previous decades such as batteries, compressed air storage, flywheels, fuel cells, hydro pumped storage, energy capacitor system (ECS), super magnetic energy storage (SMES) and so on (Tripathy et al., 1991; Chacra et al., 2005). ECS is one of the latest energy storage devices. Advantages of ECS are fast response, free maintenance, long life and

environmental friendly (Notomo et al., 2001; Qudaih et al., 2011; Yujun et al., 2014). This paper investigates the dynamics performance of both PID and H_∞-LSDP controllers and takes the advantage of the ECS in an interconnected hydro-thermal power system to improve the system stability.

According to the power fluctuation from wind energy and load variations, the development in robust control theory has provided powerful tools such as H_2, H_∞ and mixed H_2/H_∞ techniques for power system load frequency control design. The resulting robust control can play an important role in system security and reliable operation. The main target of robust control design is to develop new load frequency control methods for multi-area power systems (Glover and McFarlane, 1989; McFarlane and Glover, 1990; Bevrani, 2009; Soumya et al., 2014). To overcome the fluctuation caused by wind energy and load variations and to improve the system stability, the ECS-based H_∞-LSDP controller is considered.

In the past, two area power systems (e.g., thermal-thermal area or hydro-thermal area) have been considered as research studies. In such a system where one of the areas is hydro and the other is either thermal or hydro, interconnected via a tie line. The speed governor acts as the primary controller which balances the generation with the demand so as to control the system frequency. Nevertheless, the secondary controller matches the frequency and tie line power on (IEEE Committee Report, 1970; IEEE PES Committee Report, 1973; IEEE PES Working Group, 1992). Automatic generation control (AGC) under analysis is composed of an interconnection of two areas. AGC of interconnected power systems is increasing significantly in modern power system. Increasing demand in power system and the complexity of load profiles have required the design of interconnected power systems. The main target of AGC system is to quickly match the generation of the system with changing load demand. So, the reliability of the power system can be improved (Green, 1996; Karnavas and Papadopoulos, 2002; Nizamuddin and Bhatti, 2014).

This paper presents the H_∞-LSDP controller design of hydro-thermal power system with the ECS. The H_∞-LSDP is designed and implemented as the proposed controller. The main purpose of H_∞-LSDP controller is to control and reduce the oscillation of the system frequency after the installation of wind turbines (WTs) and load variations. The power from WTs is applied to the system. For the performance verification, the ECS-based PID controller is selected to be the candidate for comparison with parameters optimally tuned by genetic algorithm (GA) (Chiang and Safonov, 1988) in order to compare the dynamic stability in the hydro-thermal power system (Goldberge, 1989; Dulal et al., 2012).

This article can be divided into five sections. Section 1 is the introduction which discusses the adoption of the ECS to solve the power oscillations in the power system, current status of renewable energy sources and the installation of wind energy into the system. Section 2 describes the hydro-thermal power system model in terms of the dynamic equations based on the ECS and wind energy. Then, Section 3 discusses about the robust controller design using H_∞-LSDP and the PID controller design tuned by GA. Section 4 reveals the simulation results under the conditions of 5% variation of wind power in the thermal power system, consecutively. In order to verify the performance of the H_∞-LSDP controller, the hydro power system is adjusted to 10% variation of its load while the thermal power system is adjusted to 5% variation of wind power. Finally, Section 5 is the conclusion.

2 Dynamic model of interconnected hydro-thermal power system with the ECS

Based on Figure 1, the hydro-thermal power system with ECS is implemented in both of two areas. A load variation is connected to each area. The interconnected power systems consist of different control areas that are connected though tie line in order to transfer power and improve system stability (Elgerd, 1982; Elgerd and Fosha, 1970a, 1970b).

Figure 1 Hydro-thermal power system incorporating the ECS and wind power source

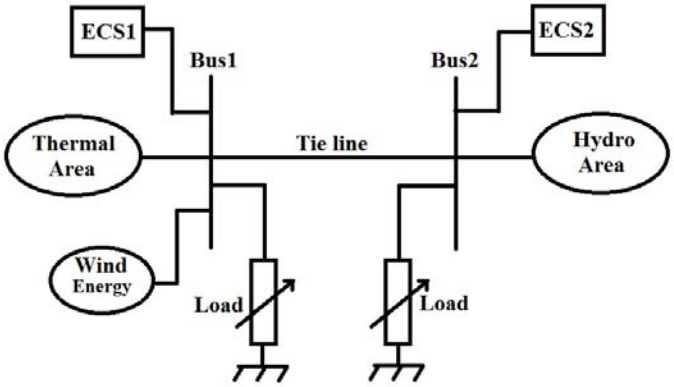

The thermal power system is consisted of the speed governor acting as a primary controller. It helps to match the generation and demand by regulating the steam input to the turbine. The reference power setting of the governor is changed by the secondary controller in order to tune the system frequency.

2.1 Thermal power system formulation

The speed governor equation is:

$$\Delta P_{G_1} = \Delta P_{ref_1} - \frac{1}{R_1}\Delta f_1 \tag{1}$$

The hydraulic amplifier equation is:

$$\Delta P_{H_1} = \left(\frac{1}{1+sT_G}\right)\Delta P_{G_1} \tag{2}$$

The non-reheat turbine equation is:

$$\Delta P_{T_1} = \left(\frac{1}{1+sT_T}\right)\Delta P_{H_1} \tag{3}$$

2.2 Hydro power system formulation

The speed governor equation is:

$$\Delta P_{G_2} = \Delta P_{ref_2} - \frac{1}{R_2}\Delta f_2 \tag{4}$$

The hydraulic amplifier equations are:

$$\Delta P_{Hg} = \left(\frac{1}{1+sT_1}\right)\Delta P_{G_2} \tag{5}$$

$$\Delta P_{H_2} = \left(\frac{1+sT_R}{1+sT_2}\right)\Delta P_{Hg} \tag{6}$$

The hydro turbine equation is:

$$\Delta P_{T_2} = \Delta P_{H_2}\left(\frac{1-sT_W}{1+0.5sT_W}\right) \tag{7}$$

The power output from the turbine becomes an input to the generator in order to feed electrical power to the system. This equation can be shown as:

$$\Delta P_{T_i} - \left(\Delta P_{D_i} + \Delta P_{ECS_i}\right) = \Delta f_i\left(\frac{K_{P_i}}{1+sT_{P_i}}\right); \quad \text{where } i = 1, 2 \tag{8}$$

The power transfer equation between two areas via tie line is expressed as:

$$\Delta P_{tie} = \frac{2\pi T_{12}}{s}\left(\Delta f_1 - \Delta f_2\right) \tag{9}$$

Because of load variations, each area experiences frequency deviation aside from tie line power deviation. This problem can be solved by using area control error (ACE). This equation followed in this paper is shown as:

$$\Delta ACE_i = \Delta P_{tie,i} + \beta_i \Delta f_i; \quad \text{where } i = 1, 2, \tag{10}$$

2.3 WT model

WT generator output is dependent on the wind speed. The characteristic of WT generator is demonstrated in Senjyu et al. (2005).

The WT system has much nonlinearity. Through the pitch controller, WT output power varies between maximum or rated power, and zero power to respond to utility grid frequency oscillations. Thus, the pitch angle set point is nonlinearly limited by these boundaries. The pitch system tunes the pitch angle and introduces nonlinearity. The WT can be simplified to a first order system. In this article, the transfer function of the WT is represented by a first-order lag (Lee and Wang, 2008) as:

$$G_{WT}(S) = \frac{K_{WT}}{sT_{WT}+1} \tag{11}$$

2.4 Energy capacitor system

ECS collects the energy in its electrostatic field created at its plates in response to resolved potential across it. Figure 2 demonstrates the structure of the ECS.

Figure 2 ECS mathematical model

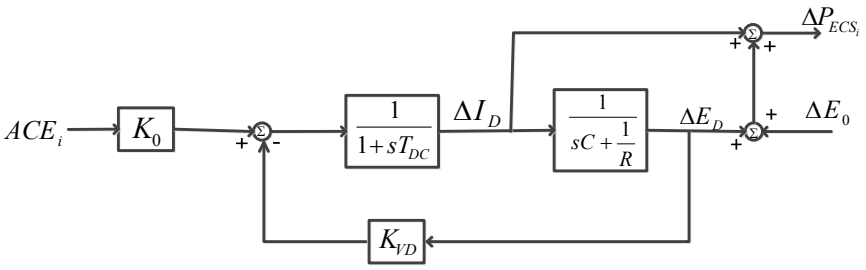

The ACE is fed as the control signal to the ECS unit. The relative equation between ACE and the ECS unit can be expressed as:

$$\Delta I_{D_i} = \left(\frac{1}{1+sT_{dc}}\right)\left(K_{ECS}\Delta ACE_i - K_{VD}\Delta E_{D_i}\right); \quad \text{where } i = 1, 2 \tag{12}$$

After a quick load variation, the restoration time of capacitor bank to normal voltage is not so fast in either of the areas. For fast restoration, a negative feedback is implemented through the voltage deviation (ΔE_D) control loop in the ECS as in Figure 2. The power output from the ECS unit is shown as:

$$\Delta P_{ECS_i} = \Delta I_{D_i}\left(E_{D_0} + \Delta E_{D_i}\right) \tag{13}$$

where

$$\Delta E_{D_i} = \frac{\Delta I_{D_i}}{C+\frac{1}{R}}; i = 1, 2 \tag{14}$$

where

- ΔP_{G_1}, ΔP_{G_2} are the governor power deviation of the thermal and hydro power system respectively
- ΔP_{ref_1}, ΔP_{ref_2} are the reference power deviation of the thermal and hydro power system respectively
- Δf_1, Δf_2 are the frequency deviation of the thermal and hydro power system respectively
- β_1, β_2 are the frequency bias constant in the thermal and hydro power system respectively
- R_1, R_2 are the regulation of speed governor constant in the thermal and hydro power system, respectively

- ΔP_{H_1}, ΔP_{H_2} are the hydraulic value power deviation of the thermal and hydro power system respectively
- ΔP_{T_1}, ΔP_{T_2} are the turbine power deviation of the thermal and hydro power system respectively
- ΔP_{Hg} is the hydro governor power deviation of the hydro power system respectively
- ΔP_{ECS_1}, ΔP_{ECS_2} are the ECS power deviation of the thermal and hydro power system respectively
- ΔP_{tie} is the tie line power deviation
- ΔP_{D_1}, ΔP_{D_2} are the load power deviation of the thermal and hydro power system respectively
- ΔACE_1, ΔACE_2 are the ACE deviation of the thermal and hydro power system respectively
- ΔI_{D_1}, ΔI_{D_2} are the current deviation of the ECS in the thermal and hydro power system respectively
- ΔE_{D_1}, ΔE_{D_2} are the voltage deviation of the ECS in the thermal and hydro power system respectively
- T_G is the governor time constant of the thermal power system
- T_T is the non-reheat turbine time constant of the thermal power system
- T_1, T_2, T_R are the time constant of the hydro governor
- T_W is the time constant of the hydro turbine
- T is the synchronising coefficient
- T_{dc} is the DC voltage time constant of the ECS unit
- T_{P_1}, T_{P_2} are the power system time constant of the thermal and hydro power system respectively
- K_{P_1}, K_{P_2} are the power system gain of the thermal and hydro power system respectively
- K_{ECS} is the ECS gain of the thermal and hydro power system
- K_{VD} is the voltage deviation gain of the ECS in the thermal and hydro power system
- C is the capacitor of the ECS
- R is the resistance of the ECS
- K_{WT} is the gain of the WT transfer function
- T_{WT} is the time constant of the WT transfer function.

Linearising (1) to (13), the resulting state space equation can be expressed as:

$$\dot{X} = AX + BU + CP \tag{15}$$

where X, U and P are:

$$X = \left[\Delta f_1 \quad \Delta f_2 \quad \Delta P_{T_1} \quad \Delta P_{T_2} \quad \Delta P_{Hg} \quad \Delta P_{H_1} \quad \Delta P_{H_2} \quad \Delta P_{tie} \quad \Delta I_{D_1} \quad \Delta I_{D_2} \quad \Delta E_{D_1} \quad \Delta E_{D_2}\right]^T$$

$$U = \left[\Delta P_{C_1} \quad \Delta P_{C_2}\right]^T$$

$$P = \left[\Delta P_{D_1} \quad \Delta P_{D_2}\right]^T$$

The modified hydro-thermal power system including the ECS and wind power source is linear and can be shown in Figure 3. The values of parameters are shown in Appendix.

Figure 3 The modified hydro-thermal power system including the ECS and wind power source (see online version for colours)

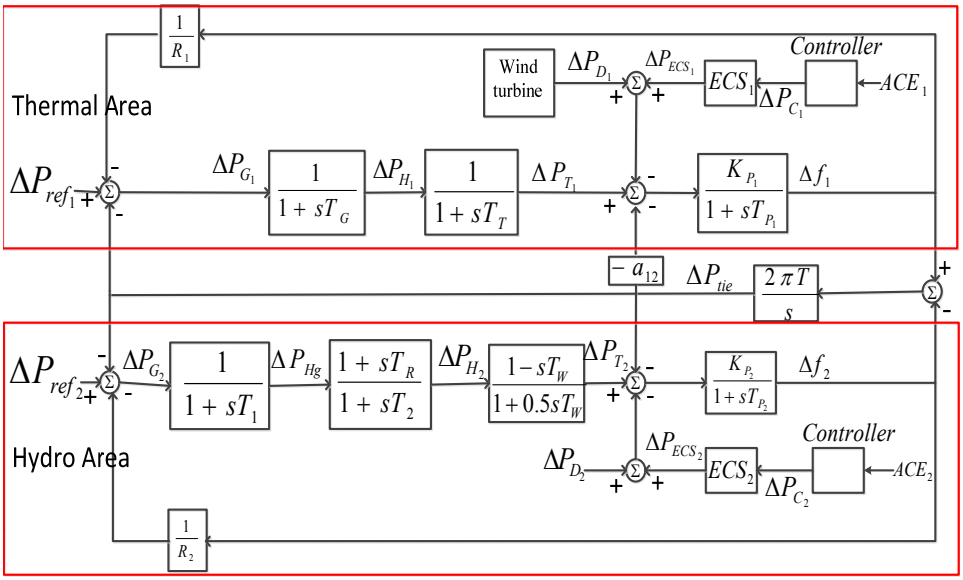

3 Proposed control strategy

3.1 Robust controller designed by H_∞-LSDP

The nominal plant of the system is G. There are two weighting functions W_1 (i.e., the lead compensation) and W_2 (i.e., the lag compensation). The shaped plant $G_S = W_2GW_1$ is enclosed by the solid line and the proposed robust controller $K_C = W_1K_\infty W_2$ is enclosed by the dashed line as shown in Figure 4.

K_∞ is the H_∞-LSDP transfer function. The weighting functions are W_1 and W_2 which are selected based on the frequency response. The purpose is to make the gain of sensitivity function small at low frequency (Glover and McFarlane, 1989).

Figure 4 Plant G_S and the robust controller design

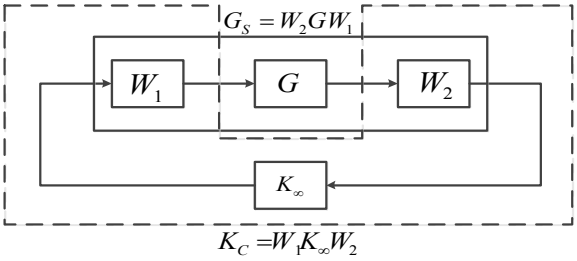

The next process of designing H_∞-LSDP is shaping the plant G_S using the left co-prime of the nominal plant $G_s = M_l^{-1} N_l$ where G_P is expressed as:

$$G_p = \left\{ \left(M_l + \Delta_M \right)^{-1} \left(N_l + \Delta_N \right) : \left\| \Delta_N \quad \Delta_M \right\|_\infty \le 1/\gamma \right\} \tag{16}$$

where ΔM and ΔN are the uncertainty transfer functions in the nominal plant G.

From the stability definition of H_∞-LSDP, G_P and K_C can be synthesised as in Figure 5. The objective function of the robust controller design does not only provide stability to the plant G, but also keeps the stability of G_P of $1/\gamma$ as in equation (16) which is the robust stability index.

The robust stability margin of the power system with uncertainty is specified by the minimum value of γ, that is $\gamma_{\min}$. Thus, $\gamma_{\min}$ is the uncertainty of the power system having the maximum size that can be closed-loop stabilised as in Figure 5. The $\gamma_{\min}$ can be calculated as follows:

$$\gamma_{\min} = \sqrt{1 + \lambda_{\max} \left(XZ \right)} \tag{17}$$

where $\lambda_{\max}(XZ)$ is the maximum value of XZ for the minimal state space realisation (A, B, C, D) of the nominal plant G. The values of X and Z are unique positive solutions to the generalised control algebraic Riccati equation.

Figure 5 Robust stability problem H_∞-LSDP

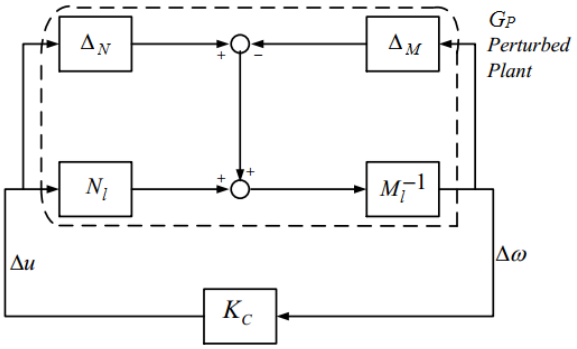

The generalised control algebraic Riccati equation.

$$\left(A - BS^{-1} D^T C \right)^T X + X \left(A - BS^{-1} D^T C \right) - XBS^{-1} B^T X + C^T R^{-1} C = 0 \tag{18}$$

The generalised filtering algebraic Riccati equation.

$$\left(A - BS^{-1}D^{T}C\right)^{T} Z + Z\left(A - BS^{-1}D^{T}C\right)^{T} - ZC^{T}R^{-1}CZ + BS^{-1}B^{T} = 0 \tag{19}$$

where $R = I + DDT$ and $S = I + DTD$. In order to ensure the robustness stability of the nominal plant G, the weighting function is selected so that $1 \le \gamma_{\min} < 4.0$ (Glover and McFarlane, 1989).

The robust controller gain can be designed from (20).

$$K_{\infty} = \begin{bmatrix} A + BF + \gamma^{2}\left(L^{T}\right)^{-1} ZC^{T}\left(C + DF\right) & \gamma^{2}\left(L^{T}\right)^{-1} ZC^{T} \\ B^{T}X & -D^{T} \end{bmatrix} \tag{20}$$

where $F = S^{-1}(D^{T}C + B^{T}X)$ and $L = (1 - \gamma^{2})I = XZ$.

Finally, the robust controller $K_C = W_1 K_{\infty} W_2$ must be conformed to the condition of:

$$\left\| \begin{bmatrix} I \\ K_{\infty} \end{bmatrix} \left(I - G_S K_{\infty}\right)^{-1} \begin{bmatrix} I & G_S \end{bmatrix} \right\|_{\infty} \le \gamma \tag{21}$$

Due to the large power system, the designed controller is normally in a very high order. Thus, the obtaining controller order needs to be reduced by using the appropriate reduction algorithm in robust control toolbox of MATLAB (Chiang and Safonoy, 1988).

3.2 PID controller with parameters optimally tuned by GA

The proportional-integral-derivative controller (PID controller) is a control loop feedback widely used in industrial and power plant control system. Thus, this paper selected it as the comparator in order to compare the results with the proposed controller.

GA is stimulated by the basic principles of natural development. GA works with a group of population of candidate solutions represented by group of chromosomes. The initial population consists of generated individuals. The fitness function of each individual is calculated in the current position of every iteration. The population is adjusted in stages to generate a new population for next iteration. The adjustment is done in three steps. The first is selection, the second is crossover; and the third is mutation. In the first process, selection is implemented as many times as there are individuals in the population. In the next process, crossover is applied by selection and combination of new individuals. The combination is done by random selection. In the final process, mutation changes the values in a randomly selected position on an individual. This process continues until one of the stopping conditions are met or global minimum is reached. Moreover, as GA does not require any information about structure of the function to be optimised and it is quick to implement (Goldberge, 1989; Dulal et al., 2012). Thus, this paper used GA in the tuning procedure to find the suitable parameters of K_P, K_I and K_D. From Figure 6, the inputs of controller are ACE_1, ACE_2 and the outputs of controller are ΔPC_1, ΔPC_2.

The performance index or fitness function is formulated by the integral time domain. The fitness function (J) is applied for optimising the gain of the PID controller and this can be expressed as:

$$\text{Minimise} \quad J = \int_0^t \left(\Delta f_1^2 + \Delta f_2^2 + \Delta P_{tie}^2 \right) \cdot tdt \tag{22}$$

Under the constraints of:

$$K_{P_{\min}} \le K_P \le K_{P_{\max}}$$
$$K_{I_{\min}} \le K_I \le K_{I_{\max}}$$
$$K_{D_{\min}} \le K_D \le K_{D_{\max}}$$

where K_P, K_I and K_D correspond to the PID controller gains of the thermal and hydro power system. The GA tool provided in MATLAB 2010 is used for optimising the fitness function (J).

Figure 6 Structure of the supplementary PID controller

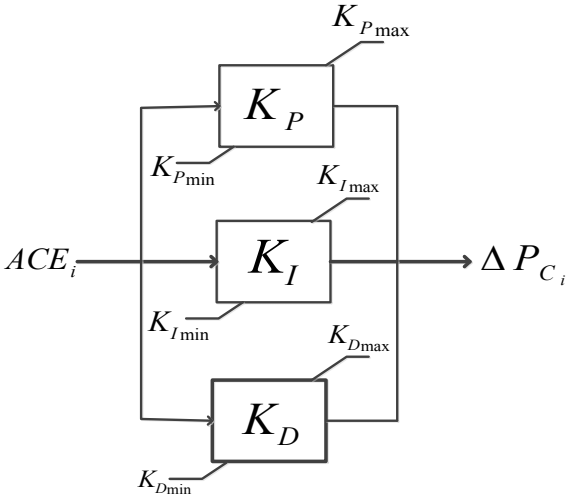

4 Simulation results

This paper makes the comparison between the hydro-thermal power system without the ECS and another one equipped the ECS-based H_∞-LSDP controller so as to illustrate the efficiency of the proposed method. The performance verification is compared against the ECS-based PID controller tuned by GA. The WTs which add to the thermal power system as the disturbance are shown in Figure 7.

The K_∞ of ΔP_{ref1} is evaluated by the ECS-based H_∞-LSDP controller which can be shown as follows:

- Controller ΔP_{C_i} :

$$K_\infty = \frac{2154}{s+63} - \frac{12}{s+0.30} + \frac{0.20}{s+0.10} \tag{23}$$

- Weighting function:

$$W_1 = \frac{50s+5}{s+0.3}, W_2 = 1 \tag{24}$$

Figure 7 Disturbance from the WTs

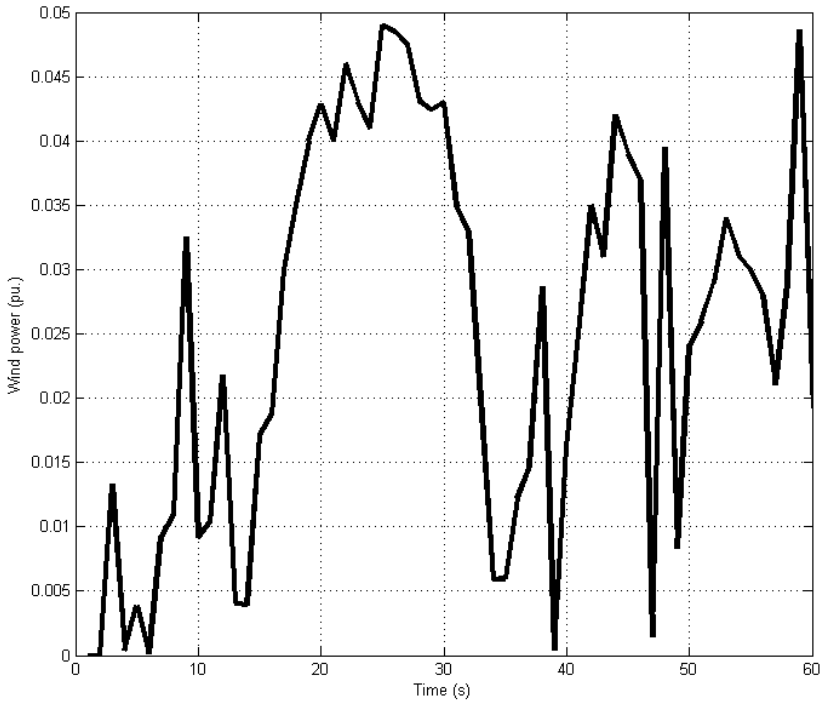

Table 1 shows the optimal values of PID controllers which tuned by GA.

Table 1 Parameters used in the PID controllers

PID controller	*KP*	*KI*	*KD*
Thermal area	0.59	–0.05	–0.12
Hydro area	–0.45	–0.06	0.53

Based in Figure 8, the magnitude and phase of the frequency response without the H_∞-LSDP controller have less damping which yield to resonance peak of 9 dB and 630 deg, respectively. After including the H_∞-LSDP controller, the resonance peak of the magnitude and phase is decreased in Figure 8.

Based on the simulation results, the wind power is increased by 5%the installed capacity of the thermal power system. In this case, a variation in the generated electrical

power of the system is also increased, which consequently affects the frequency of the power system. The frequency and power responses of the hydro-thermal power system are presented in Figures 9 to 13 accordingly. From the figures, it can be seen that the ECS-based H_∞-LSDP controller can overcome fluctuations caused by 5% variation of wind power better than the hydro-thermal power system with the ECS-based PID controller. Hence, the results of the ECS-based H_∞-LSDP controller indicate a more desirable performance as compared to the ECS-based PID controller.

Figure 8 Frequency response of the hydro-thermal power system with the ECS designed by H_∞-LSDP

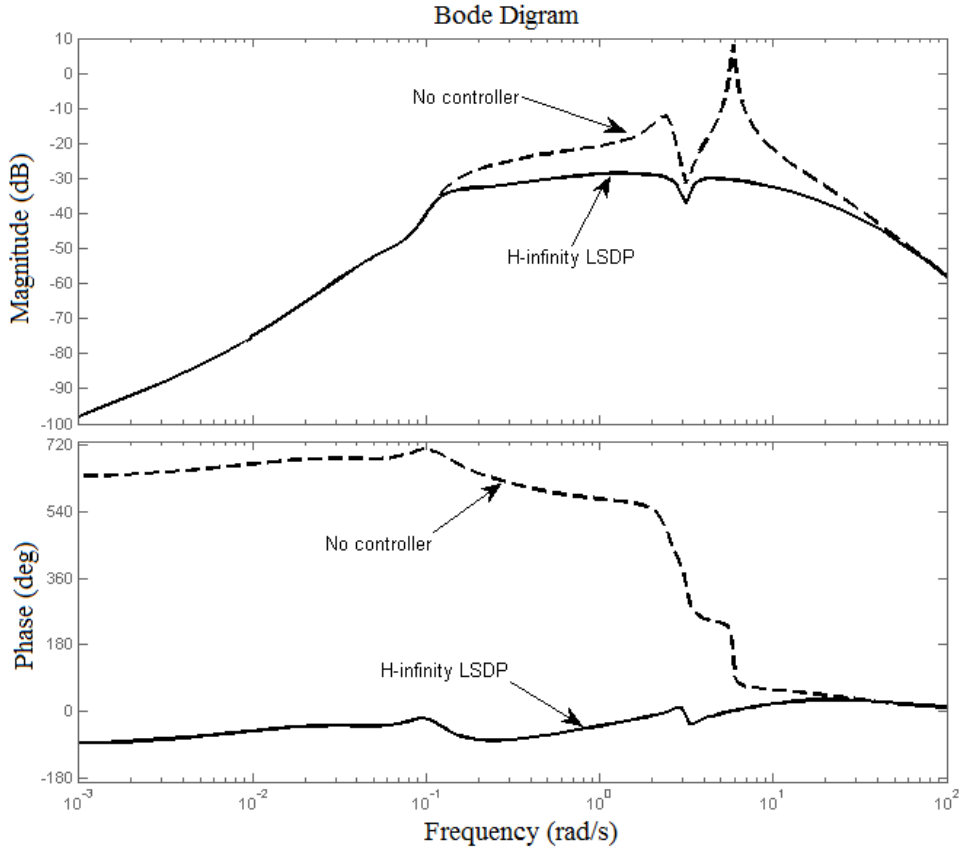

The hydro power system is adjusted to 10% variation of its load while the thermal power system is adjusted to 5% variation of wind power so as to show the robustness of the ECS-based H_∞-LSDP controller. The frequency and power responses of the hydro-thermal are shown in Figures 14 to 18. From these figures, it is clear that the ECS-based H_∞-LSDP controller can still preserve the stability better than the ECS-based PID controller.

Figure 9 Frequency response of the thermal power system with 5% variation of the wind power

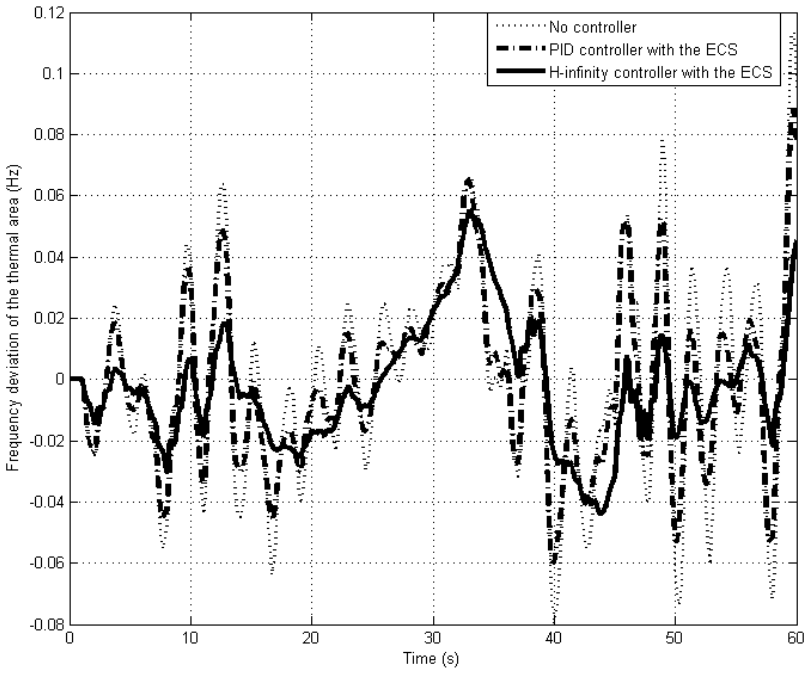

Figure 10 Frequency response of the hydro power system with 5% variation of the wind power

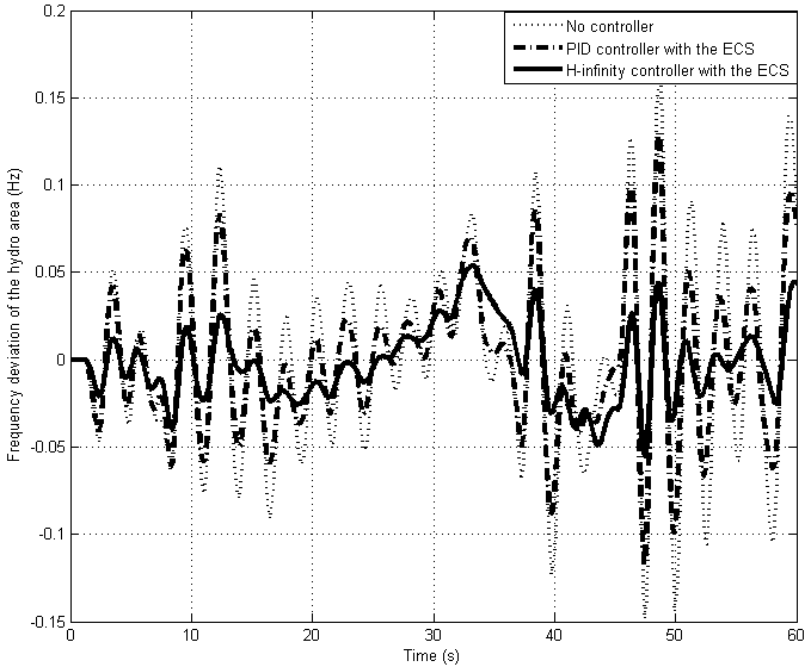

Figure 11 Tie line power response of the hydro power system with 5% variation of the wind power

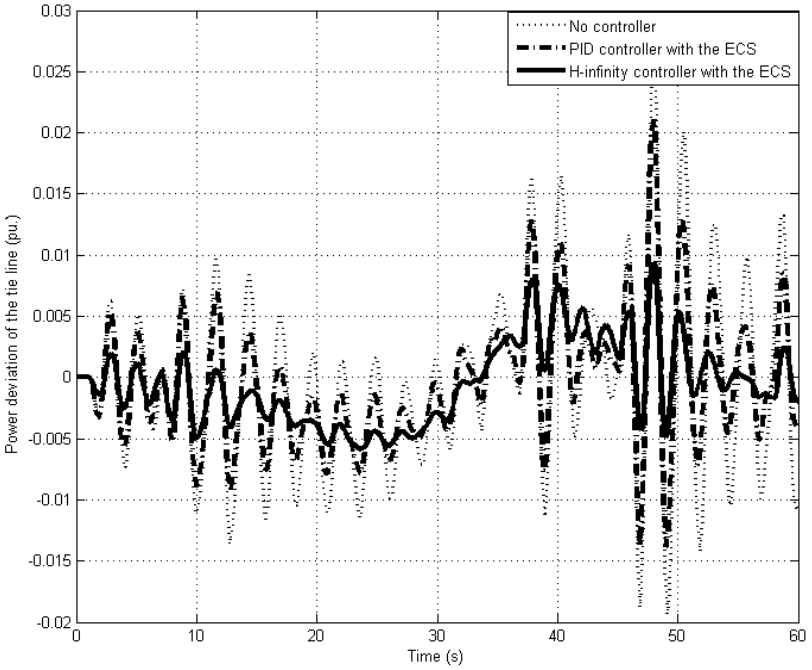

Figure 12 Power response of the thermal power system with 5% variation of the wind power

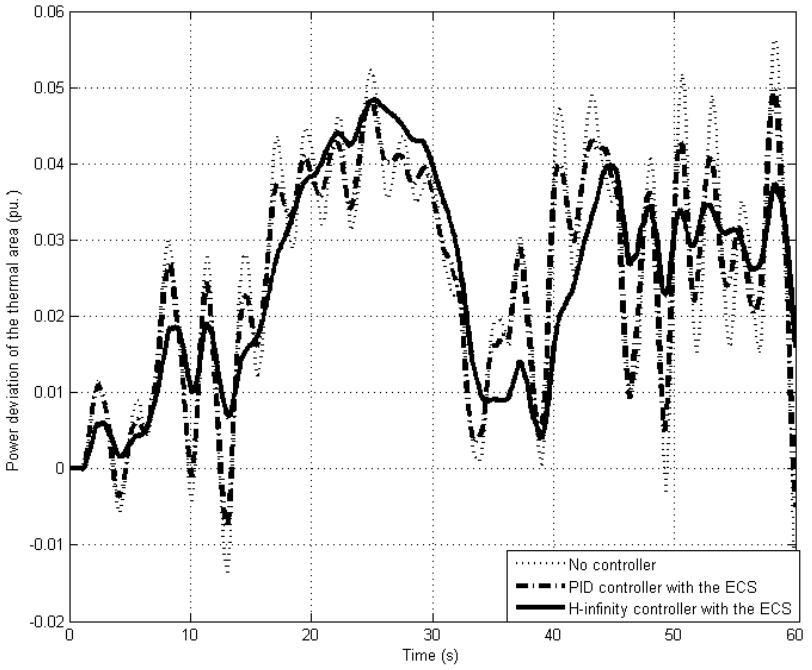

Figure 13 Power response of the hydro power system with 5% variation of the wind power

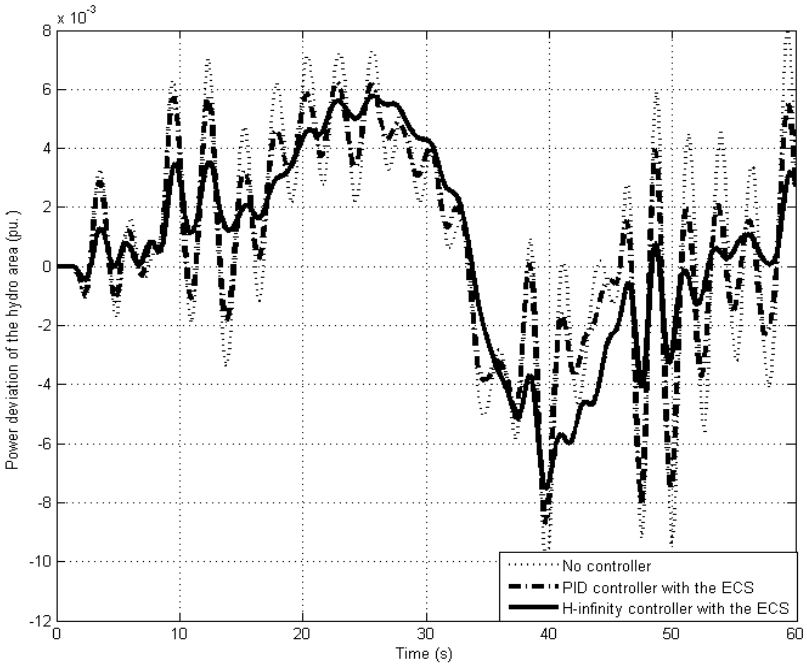

Figure 14 Frequency response of the thermal power system with 5% variation of the wind power and 10% variation of load in the hydro power system

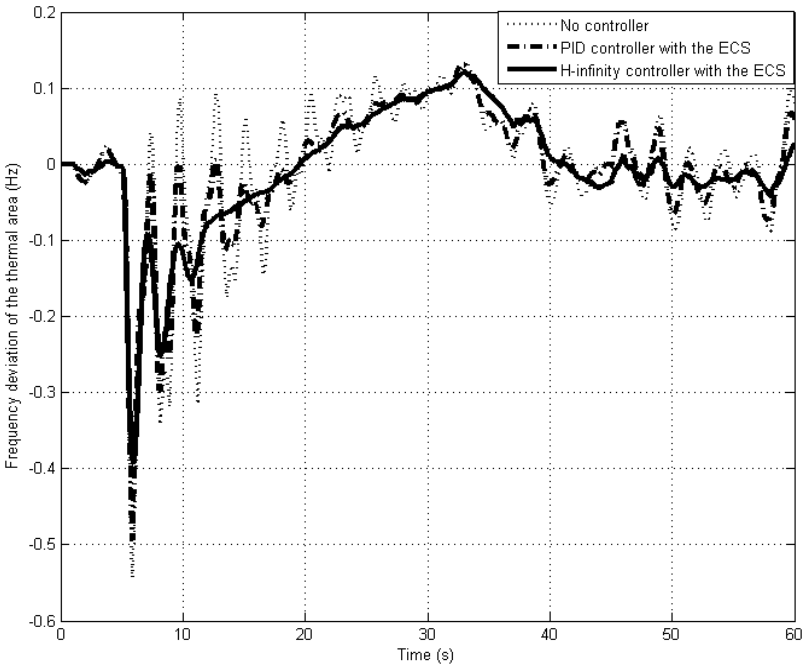

Figure 15 Frequency response of the hydro power system with 5% variation of the wind power and 10% variation of load in the hydro power system

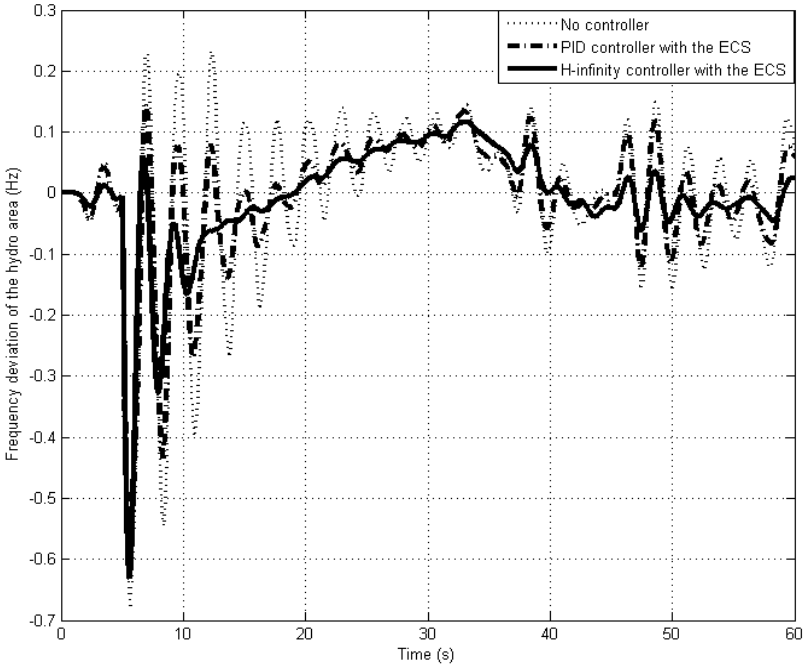

Figure 16 Power response of the tie line with 5% variation of the wind power and 10% variation of load in the hydro power system

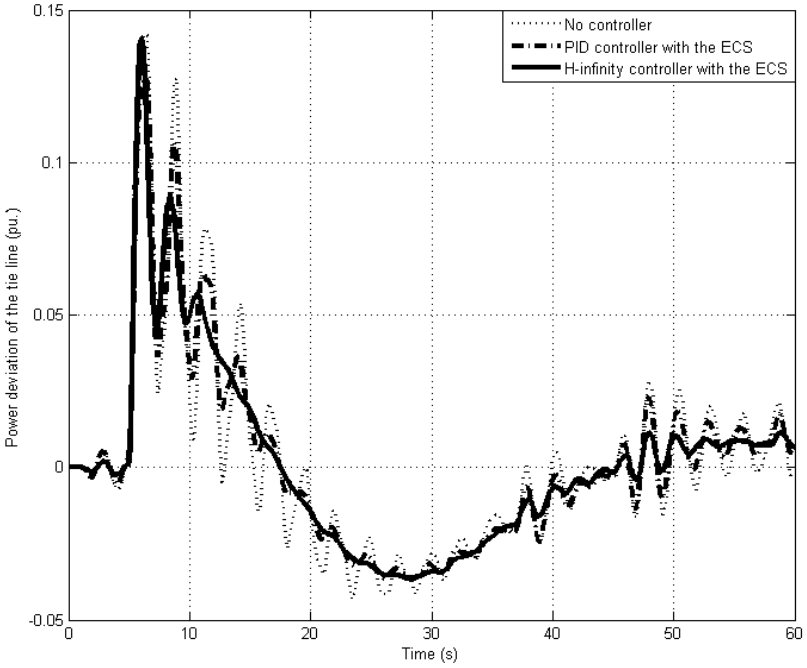

Figure 17 Power response of the thermal power system with 5% variation of the wind power and 10% variation of load in the hydro power system

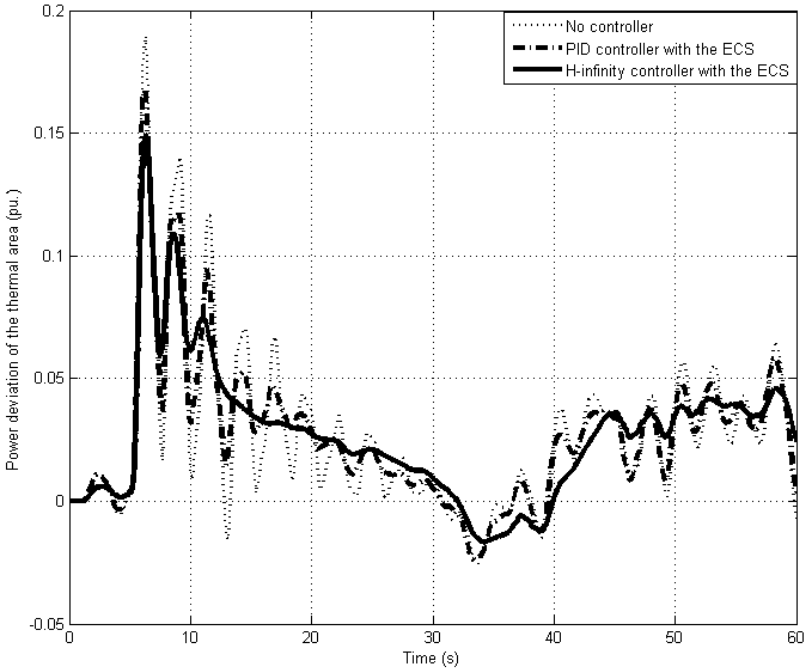

Figure 18 Power response of the hydro power system with 5% variation of the wind power and 10% variation of load in the hydro power system

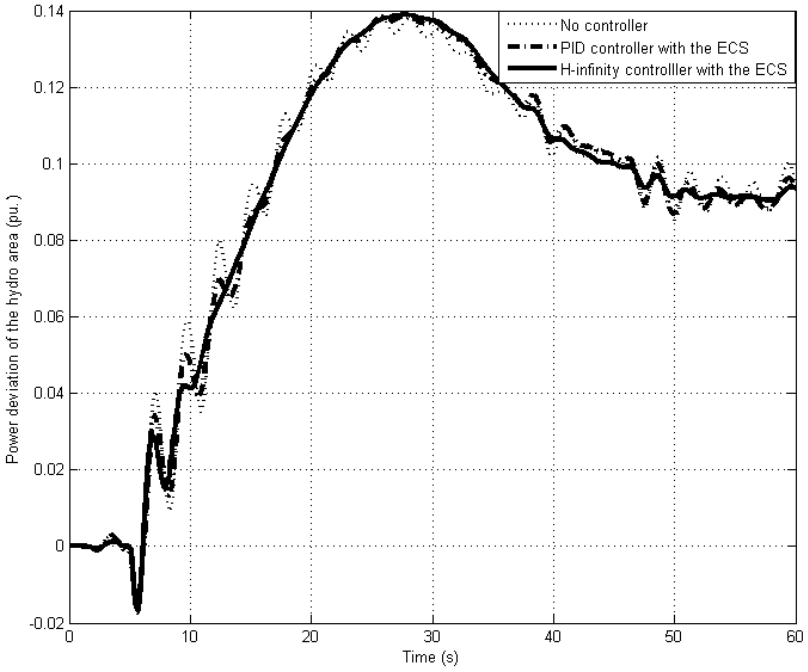

5 Conclusions

The robust hydro-thermal power system controller design with the ECS is proposed in order to improve system stability under wind power disturbance with 5% variation of installed capacity. In this paper, the performance of controller is compared with the ECS-based PID controller. The results are shown that the ECS-based H_∞-LSDP controller provides smooth and robust system stability compared to the ECS-based PID controller. After the hydro power system has been adjusted to 10% of its load, the ECS-based H_∞-LSDP controller can still preserve the performance better than the ECS-based PID controller. Moreover, it has been shown that the system frequency and tie line power oscillations caused by the variations of wind power and loads can be reduced in both the areas by the ECS-based H_∞-LSDP controller. Therefore, the AGC performance of hydro-thermal power system can be improved by the ECS-based H_∞-LSDP controller.

References

Bevrani, H. (2009) *Robust Power System Frequency Control*, Springer, Germany.

Chacra, F., Bastard, P., Fleury, G. and Clavreul, R. (2005) 'Impact of energy storage costs on economical performance in a distribution substation', *IEEE Trans. Power System*, Vol. 20, No. 2, pp.684–691.

Chiang, L.Y. and Safonov, M.G. (1988) *Robust Control Toolbox*, MathWorks, South Natick, MA.

Dulal, D., Roy, A. and Sinha, N. (2012) 'GA based frequency controller for solar thermal-diesel-wind hybrid energy generation/energy storage system', *Int. J. Electr. Power Energy Syst*., Vol. 43, No. 1, pp.262–279.

Elgerd, O.I. (1982) *Electric Energy Systems Theory: An Introduction*, 2nd ed., McGraw-Hill, New York, NY.

Elgerd, O.I. and Fosha, C. (1970a) 'Optimum megawatt-frequency control of multiarea electric energy systems', *IEEE Trans. Power Apparatus System*, Vol.PAS-89, No. 4, pp.556–563.

Elgerd, O.I. and Fosha, C. (1970b) 'The megawatt-frequency control problem: a new approach via optimal control', *IEEE Trans. Power Apparatus System*, Vol. PAS-89, No. 4, pp.563–577.

Francisco, D., Malanie, H., Andreas, S. and Oriol, G. (2015) 'Coordinated operation of wind turbines and flywheel storage for primary frequency control support', *Int. J. Electr. Power Energy Syst*., Vol. 68, No. 1, pp.313–326.

Glover, K. and McFarlane, D (1989) 'Robust stabilization of normalized coprime factor plant description with H_∞-bounded uncertainty', *IEEE Trans. Automatic Control*, Vol. 34, No. 8, pp.821–830.

Goldberge, D.E. (1989) *Genetic Algorithm in Search, Optimization and Machine Learning*, Addison-Wesley Publishing Company Inc., USA.

Green, R.K. (1996) 'Transformed automatic generation control', *IEEE Trans. Power Systems*, Vol. 11, No. 1, pp.1799–1804.

Gu, W., Wang, R., Sun, R. and Li, Q. (2005) 'Wind power penetration limit calculation based on stochastic optimal power flow', *International Review of Electrical Engineering (IREE)*, Vol. 6, No. 4, pp.1939–1945.

Nizamuddin, I. and Bhatti, T. (2014) 'AGC of two area power system interconnected by AC/DC links with diverse sources in each area', *Int. J. Electr. Power Energy Syst*., Vol. 55, No. 1, pp.297–304.

IEEE Committee Report (1970) 'Standard definitions of terms for automatic generation control on electrical power systems', *IEEE Trans. Electric Power Apparatus System*, Vol. 89, No. 4, pp.1356–1364.

IEEE PES Committee Report (1973) 'Dynamic models for steam and hydro turbine in power system studies', *IEEE Trans. Power Apparatus System*, Vol. 92, No. 1, pp.455–463.

IEEE PES Working Group (1992) 'Hydraulic turbine and turbine control models for system dynamics', *IEEE Trans. Power System*, Vol. 92, No. 1, pp.455–463.

Karnavas, Y.L. and Papadopoulos, D.P. (2002) 'AGC for autonomous power system using combined intelligent techniques', *International Journal of Electrical Power System Research*, Vol. 62, No. 3, pp.225–239.

Lalor, G., Mullane, A. and O'Malley, A. (2005) 'Frequency control and wind turbine technologies', *IEEE Trans. Power Systems*, Vol. 20, No. 4, pp.1905–1913.

Lee, D. and Wang, L. (2008) 'Small-signal stability analysis of an autonomous hybrid renewable energy power generation/energy storage system part I: time-domain simulations', *IEEE Trans. Energy Conversion*, Vol. 23, No. 1, pp.311–320.

McFarlane, D. and Glover, K. (1990) 'Robust controller design using normalized coprime factor plant descriptions', *Lecture Notes in Control and Information Sciences*, Vol. 138, Springer-Verlag.

Notomo, S., Nakata, H., Yoshioka, K., Yoshida, A. and Yoneda, H. (2001) 'Advanced capacitors and their application', *Journal of Power Sources*, Vol. 97, No. 1, pp.807–811.

Qudaih, Y., Elbaset, A. and Hiyama, T. (2011) 'Simulation studies on ECS application in a clean power distribution system', *Int. J. Electr. Power Energy Syst*., Vol. 33, No. 1, pp.43–54.

Senjyu, T., Nakaji, T., Uezato, K. and Funabashi, T. (2005) 'A hybrid power system using alternative energy facilities in isolated island', *IEEE Trans. Energy Conversion*, Vol. 20, No. 2, pp.406–414.

Soumya, M., Nand, K. and Prakash, R. (2014) 'Robust H-infinite loop shaping controller based on hybrid PSO and harmonic search for frequency regulation in hybrid distributed generation system', *Int. J. Electr. Power Energy Syst*., Vol. 60, No. 1, pp.302–3016.

Tripathy, S., Kalantar, M. and Balasubramanian, R. (1991) 'Dynamics and stability of wind and diesel turbine generators with superconducting magnetic energy storage unit on an isolated power system', *IEEE Trans. Energy Conversion*, Vol. 6, No. 1, pp.46–51.

Yujun, L., Zeren, Z., Yong, Y., Yingyi, L., Hairong, C. and Zheng, X. (2014) 'Coordinated control of wind farm and VSC-HVDC system using capacitor energy and kinetic energy to improve inertia level of power systems', *Int. J. Electr. Power Energy Syst*., Vol. 59, No. 1, pp.79–92.

Appendix

A System data

T_G = 0.08 s, T_T = 0.3 s, T_1 = 42.5 s, T_2 = 0.515 s, T_R = 5 s, T_W = 1 s, T = 0.0855 s, T_{dc} = 0.05 s, TP_1 = 20 s, TP_2 = 20 s, KP_1 = 120 Hz/pu, KP_2 = 120 Hz/pu, a_{12} = –1, $\beta_1 = \beta_2 = 0.424$, $R_1 = R_2 = 2.4$ Hz/pu, $P_{Thermal} = P_{Hydro}$ = 1,200 MW.

B Energy capacitor system

K_{VD} = 0.1 KV/KA, K_0 = 69 KV/Hz, C = 1 F, R = 100 Ω, ED_0 = 2 KV.